Published in final edited form as:
J Am Chem Soc. 2007 February 14; 129(6): 1733–1742. doi:10.1021/ja067800f.

Mechanistic Studies on the Galvanic Replacement Reaction between Multiply Twinned Particles of Ag and $HAuCl_4$ in an Organic Medium

Xianmao Lu[1], **Hsing-Yu Tuan**[2], **Jingyi Chen**[1], **Zhi-Yuan Li**[3], **Brian A Korgel**[2], and **Younan Xia**[1,*]

1 *Department of Chemistry, University of Washington, Seattle, Washington 98195*

2 *Department of Chemical Engineering, Texas Materials Institute and Center for Nano- and Molecular Science and Technology, University of Texas, Austin, Texas 78712*

3 *Laboratory of Optical Physics, Institute of Physics, Chinese Academy of Sciences, Beijing 100080, P. R. China*

Abstract

This article presents a mechanistic study on the galvanic replacement reaction between 11- and 14-nm multiply twinned particles (MTPs) of Ag and $HAuCl_4$ in chloroform. We monitored both morphological and spectral changes as the molar ratio of $HAuCl_4$ to Ag was increased. The details of reaction were different from previous observations on single-crystal Ag nanocubes and cubooctahedrons. Because Au and Ag form alloys rapidly within small MTPs rich in vacancy and grain boundary defects, a complete Au shell did not form on the surface of each individual Ag template. Instead, the replacement reaction resulted in the formation of alloy nanorings and nanocages from Ag MTPs of decahedral or icosahedral shape. For the nanorings and nanocages derived from 11-nm Ag MTPs, the surface plasmon resonance (SPR) peak can be continuously shifted from 400 to 616 nm. When the size of Ag MTPs was increased to 14 nm, the SPR peak can be further shifted to 740 nm, a wavelength sought by biomedical applications. We have also investigated the effects of capping ligands and AgCl precipitate on the replacement reaction. While hollow structures were routinely generated from oleylamine-capped Ag MTPs, we obtained very few hollow structures by using a stronger capping ligand such as oleic acid or tri-n-octylphosphine oxide (TOPO). Addition of extra oleylamine was found to be critical to the formation of well-controlled, uniform hollow structures free of AgCl contamination thanks to the formation of a soluble complex between AgCl and oleylamine.

1. Introduction

Nanostructures made of noble metals, silver and gold in particular, have received renewed interests in recent years owning to their interesting optical,[1] electronic,[2] and catalytic[3] properties and thus a broad range of intriguing applications including surface-enhanced Raman scattering (SERS),[4] information storage,[5] and energy conversion.[6] Many approaches have been developed to prepare silver and gold nanostructures in different shapes, including nanowires,[7] nanorods,[8] nanospheres,[9–11] nanocubes,[11,12] and nanoplates.[13] Recently, extensive efforts have been devoted to the synthesis of more complex structures – core-shell or hollow nanoparticles. Due to their increased surface areas, reduced densities, and tunable

*Corresponding author. Email: xia@chem.washington.edu.

SPR features,[14] these new types of metal nanostructures are expected to outperform their solid counterparts in applications such as optical imaging,[15] SERS,[16] and photothermal therapy.[17]

Template-directed growth has proved to be a convenient approach to the preparation of core-shell nanoparticles by depositing a thin layer of the shell material on the surface of the template, typically polymeric or silica beads. For example, Halas and co-workers have reported that Au nanoshells of different thicknesses could be grown on 120-nm silica spheres via an chemical reduction process.[18] Together with a number of studies which have also demonstrated formation of metal shells on dielectric colloidal spheres, it has been established that there was a significant red-shift for the SPR peaks relative to their solid counterparts.[19,20] By selectively removing the core through chemical etching or calcination,[20] the core-shell particle can be transformed into a hollow one with a void in the center. Because the deposited metal shells are polycrystalline, the hollow structures fabricated using this method are often bothered by issues including relatively large sizes (>100 nm), low yields, rough surfaces, poor control, limited scope of tuning, and structural fragility.

Previously, we have demonstrated that hollow nanostructures of various noble metals could be synthesized via galvanic replacement reaction in an aqueous solution by reacting sacrificial Ag template with a precursor compound of the desired metal such as Au, Pd, or Pt. For example, Ag templates with a variety of shapes, including nanocubes, nanoplates, nanospheres, nanorods, and nanowires, could react with $HAuCl_4$ in an aqueous medium to generate nanoboxes,[12a,21a–c] nanocages,[17] nanorattles,[21d] and nanotubes[21d,e] in a single step. The SPR band of resultant hollow structures could be readily engineered to the near infrared region (800–1200 nm) by controlling the volume of $HAuCl_4$ solution added to the suspension of Ag templates, and consequently the thickness, porosity, and elemental composition of the wall. This synthetic strategy has also been successfully applied to both Pt and Pd with appropriate precursors to the metals.[21f] Most recently, this water-based synthetic route was also extended to organic media. To this end, Selvakannan and Sastry performed the replacement reaction by transferring both suspension of Ag nanoparticles and $HAuCl_4$ solution from water into chloroform through phase transfer ligands and obtained Au or Pt hollow nanoparticles with SPR peaks red-shifted to ~570 nm.[14] Yang and co-workers reported that by following a slightly modified method, Ag-Au core-shell nanoparticles were obtained from the reaction between 9.6-nm Ag nanospheres and dodecylamine-hydrophobized $HAuCl_4$ in toluene.[22] Another study from the Alivisatos group showed that the replacement reaction between $AuCl_3$ and single-crystal Ag cubooctahedrons in o-dichlorobenzene resulted in the epitaxial growth of Au on the {100} facets of Ag template.[23]

Synthesis of hollow structures in an organic phase may provide an attractive route to optical coatings by spray-deposition,[14] be more amenable for subsequent surface modification,[22] and add greater value to catalytic applications.[24] There is also demand to use Ag nanoparticles <20 nm in size as the sacrificial template because many applications could be greatly enhanced by reducing the dimensions of the hollow structures. For instance, when used as SERS probes or imaging contrast agents, hollow structures of compact sizes would substantially render their accessibility to subcelluar organelles, as well as to speed up their diffusion in tissues.[16] Silver nanoparticles <20 nm in size can be prepared as monodispersed samples using a number of methods. These small particles usually exist as MTPs in the decahedral or icosahedral shape.[25] Although we reported two years ago a mechanistic study on the galvanic replacement reaction between single-crystal Ag nanocubes and $HAuCl_4$ in an aqueous medium,[21c] it is still not clear how Ag MTPs behave when they react with $HAuCl_4$ in an organic medium. Due to the rich vacancy and grain boundary defects and the rapid diffusion rate of atoms in small particles, Ag MTPs are expected to behave quite differently from single-crystal Ag nanocubes in a galvanic replacement process. Herein we present a systematic study on the galvanic replacement reaction between 11- and 14-nm Ag MTPs and $HAuCl_4$ in chloroform. The Ag

MTPs were synthesized in an organic phase in the presence of oleylamine. Different from the replacement reaction of Ag nanocubes (which forms single-crystal nanoboxes and nanocages through interplay of epitaxial growth of Au on the Ag template, alloying, and dealloying), the morphological evolution of Ag MTPs follows a distinct pathway. When they were titrated with $HAuCl_4$ in chloroform, instead of forming complete shell, the Ag MTP evolved into a nanoring or nanocage in the course of galvanic replacement, alloying, and dealloying, with the SPR peak tunable to 740 nm for the 14-nm Ag MTPs. Addition of extra oleylamine was found to be critical to the formation of well-defined, uniform hollow structures free of AgCl contamination by forming a soluble complex between AgCl and oleylamine during the replacement reaction. We further examined the effects of capping ligands on the replacement reaction. Although oleylamine-capped Ag MTPs could be transformed into hollow structures with a yield approaching 100%, very few hollow structures were observed when oleylamine was replaced by stronger capping ligands such as oleic acid and TOPO. Combined together, this work has greatly advanced our understanding on the galvanic replacement reaction that involves the use of Ag MTPs <15 nm in size and an organic medium.

2. Experimental

Preparation of Silver MTPs

Silver MTPs of two different sizes, 11 and 14 nm in diameter, were synthesized through the decomposition of silver trifluoroacetate (99.99+%, Aldrich) in o-dichlorobenzene (ODCB, 99%, Aldrich) or isoamyl ether (99%, Aldrich) in the presence of oleylamine (70%, Aldrich). In a typical synthesis of 11-nm Ag MTPs, 0.055 g silver trifluoroacetate (0.25 mmol) was dissolved in 1 mL ODCB at 50 °C with magnetic stirring for 30 min. The solution was mixed with 0.25 mL oleylamine and then injected into 3 mL of ODCB, which had been heated to 180 °C in a 25 mL 3-neck flask with a heating mantle under continuous flow of argon. The temperature of the mixture was monitored with a thermal couple connected to a temperature controller. Upon injection, the temperature dropped to 150 °C and then rose to 180 °C in 5 min. The color of the solution changed from clear to brown gradually. After 60 min, the reaction was stopped by removing the heating mantle and allowed to cool down to room temperature. The product was precipitated out from the reaction mixture by adding 10 mL of ethanol, followed by centrifugation at 3,900 rpm for 5 min. The precipitate was washed with 5 mL of ethanol and then dispersed in 5 mL of hexane. Silver MTPs of 14 nm in diameter were obtained by mixing 0.22 g silver trifluoroacetate (1 mmol), 5 mL of isoamyl ether, and 0.66 mL of oleylamine (2 mmol) and then heating up to 160 °C in 80 min. After staying at 160 °C for 1 h, the product was collected and washed following the procedure for the 11-nm MTPs and finally dispersed in 20 mL of chloroform.

Ligand Exchange

Ligand exchange was performed on the 11-nm Ag MTPs capped by oleylamine with two other capping ligands: oleic acid (70%, Aldrich) and tri-n-octylphosphine oxide (TOPO, 99%, Aldrich). Silver MTPs capped with oleic acid and TOPO were obtained by adding 0.15 mL oleic acid (0.4 mmol) and 0.15 g TOPO (0.4 mmol), respectively, to 2 mL oleylamine-capped Ag MTPs dispersed in hexane, followed by sonication for 30 min. The product was collected by centrifugation at 3,900 rpm for 5 min, washed twice with 10 mL of ethanol, and finally dispersed in 2 mL of $CHCl_3$.

Galvanic Replacement Reaction

A 0.5 mM solution of chloroauric acid ($HAuCl_4{\cdot}3H_2O$, 99.9+%, Aldrich) was prepared by dissolving 2 mg $HAuCl_4{\cdot}3H_2O$ in 10 mL of $CHCl_3$. A 25 mL flask was loaded with 0.2 mL of the 11-nm Ag MTPs (or 50 μL for 14-nm Ag MTPs) suspended in $CHCl_3$. The dispersion was then diluted to 5 mL with $CHCl_3$, followed by addition of 200 μL oleylamine. After heating

to 50 °C using oil bath under magnetic stirring, the 0.5 mM $HAuCl_4$ solution in $CHCl_3$ was injected with a syringe pump (KDS-200, Stoelting, Wood Dale, IL) at an injection rate of 0.2 mL/min. The color of the solution changed gradually from yellow to green, brown, violet, and stopped at blue as $HAuCl_4$ was injected. If excess $HAuCl_4$ was injected, the color turned into red, indicating that Au solid nanoparticles were formed. Upon completion of the reaction, the product was precipitated out with ethanol, followed by centrifugation and then re-dispersed in hexane.

Instrumentation

Transmission electron microscopy (TEM) studies were done with a Philips EM420T microscope operated at 120 kV by drop casting the particle dispersions on copper grids coated with formvar and carbon film (SPI, West Chester, PA). High-resolution TEM (HRTEM) images were obtained with a JEOL 2010F microscope operated at 200 kV accelerating voltage. Electron dispersive X-ray spectroscopy (EDX) was performed on the JEOL 2010F TEM with an Oxford spectrometer. UV-visible (UV-vis) absorption spectra were taken on a Hewlett-Packard 8452A spectrometer using quartz cuvettes with an optical path length of 1 cm. Fourier Transform Infrared (FTIR) spectra were collected with a Brucker Vector 33 IR spectrometer. FTIR samples were prepared by drop casting nanoparticles dispersions on KBr pellets, followed by drying in vacuum. Powder X-ray diffraction (XRD) was performed on a Philips 1820 X-ray diffractometer with Cu *K*α radiation and the sample was deposited onto a glass slide.

3. Results and Discussion

Morphology of the Silver MTPs before and after Galvanic Replacement Reaction

Figure 1A shows a typical TEM image of the Ag nanoparticles with an average diameter of 11.2 nm and a polydispersity of ~10%. The inhomogeneous contrast within each nanoparticle shown on the TEM image indicates polycrystallinity, which is also supported by HRTEM (Figure 1C). Two types of multiple twinned structures – decahedron and icosahedron, commonly referred to as MTPs, were revealed from the HRTEM images (Figure S2), consistent with the observation for small Ag nanoparticles reported by various research groups.[10,26] Both MTPs can be considered as the twinned assembly of a number of tetrahedra – 5 for decahedron and 20 for icosahedron, respectively. Due to the boundary gaps between tetrahedrons within each MTP, lattice distortion and high strain at the apexes and ridges of the particles are expected.[27] For non-truncated Ag MTPs with a decahedral or icosahedral shape, the entire surface is covered by {111} facets,[27,28] leading to a stable structure with the lowest surface energy. When truncated, however, other facets, such as {110} and {100}, can be developed on the ridges and apexes as well. The as-synthesized Ag nanoparticles in this study exhibited a spherical profile, indicating some degree of truncation.

Figure 1B shows the product derived from the galvanic replacement reaction between the 11-nm Ag MTPs and 2.6 mL of 0.5 mM $HAuCl_4$ in $CHCl_3$. All the particles have hollow interiors, with an average size of 12.4±1.1 nm in diameter, 12% bigger than the original Ag MTPs. The HRTEM in Figure 1D implies that the hollow particles are characterized by a ring-type structure. The thickness of the rings ranges from 2.5 to 5.5 nm with an average around 4.5 nm. This value is a rough estimate since the thickness also varies within each individual particle. The hollow particles also show polycrystallinity with various lattice planes clearly revolved on the HRTEM image. EDX taken from single particles (Figure S3) indicate that they were composed of a Au-Ag alloy, with a Ag to Au atomic ratio of 2:1, indicating that only 60% of the Ag in the starting MTP was replaced with Au, based on the fact that Ag reacts with $HAuCl_4$ at a atomic ratio of 3:1.

Figure 2 details the morphological evolution of the 11-nm Ag MTPs before and after adding different volumes of the $HAuCl_4$ solution. Before any $HAuCl_4$ was added, the Ag MTPs were spherical with butterfly-like contrast under TEM (Figure 2A), indicating that these particles had a multiple twinned structure and possibly rounded off by truncation on the edges and apexes. After adding 1 mL of 0.5 mM $HAuCl_4$ solution, the average size of the Ag particles increased from 11.2 to 12.3 nm in diameter. Although some particles appeared to be unchanged, about 30% of them exhibited a small pinhole due to the oxidation of Ag by $HAuCl_4$ (Figure 2B). With more $HAuCl_4$ solution (2.0 mL) added, enlargement of the pinholes or multiple holes were observed on the Ag nanoparticles (Figure 2C). The holes on some nanoparticle were separated by ridges, making them appear like nanocages with holes on the shell. The particle showed a rough surface due to the growth and etch taking place at different regions of the particle. After 2.6 mL $HAuCl_4$ solution had been injected, the nanoparticles evolved into ring-like structures, as revealed by the TEM image in Figure 1B and HRTEM image on Figure 1D. Although ~10% of the voids appeared in the center of the particles, most of them were not centered, resulting in non-uniformity for the shell thickness. If the volume of $HAuCl_4$ solution was further increased to 3.1 mL, the nanorings would start to break and/or collapse due to dealloying, forming smaller solid Au particles with sizes ranging from 3 to 10 nm (Figure 2D).

Figure 3 shows TEM images of a product obtained by reacting the 14-nm Ag MTPs with 1.2 mL of 0.5 mM $HAuCl_4$ solution in $CHCl_3$. The size of the particles increased to 15.2±2.1 nm with 75% of the hollow particles showing a cage-like structure. Figure 3B shows HRTEM image of a single nanocage, indicating that even though lattice fringes were missing in some areas, the apexes of the particles were well preserved. This result suggests that the oxidation of Ag might preferentially start from the {111} facets of each MTP, rather than the twin boundaries.

Reaction Mechanism

We previously found that the galvanic replacement reaction for 100-nm Ag nanocubes in an aqueous solution involved a two-step alloying-dealloying process: *i*) formation of pin-hole free nanoboxes made of Ag/Au alloys as the intermediate product; and *ii*) formation of Au nanocages with porous walls through dealloying.[21b,c] In a recent study on the galvanic replacement reaction of single-crystal Ag cubooctahedrons in o-dichlorobenzene, Alivisatos and co-workers observed formation of faceted hollow Au nanocrystals due to the selective etching and growth taking place at faces of different lattice planes. In the present work, we found that the morphological evolution of 11-nm and 14-nm Ag MTPs took a third different path when subjected to a galvanic replacement reaction with $HAuCl_4$ in $CHCl_3$. For comparison, these three different mechanisms are collected in Figure S1.

In general, the galvanic replacement reaction between a Ag template and $HAuCl_4$ involves a number of processes, including diffusion of $HAuCl_4$ to the surface of the template, diffusion of Ag atoms from bulk to surface, formation of Ag^+ and Au species, deposition of Au atoms on the surface of template, and alloying or dealloying between Au and Ag depending on the volume of $HAuCl_4$ solution added. It has been established that the replacement reaction should start from the highest energy sites, usually those with step or point defects or stacking faults.[29] For the Ag MTPs enclosed by {111} facets, the highest energy sites should be mainly located at the ridges and apexes, since they are formed from twinned defects with lattice distortion. TEM analysis on the particles with pinholes (formed after adding 2.0 mL of $HAuCl_4$ to the 11-nm Ag MTPs, or 1.2 mL of $HAuCl_4$ to the 14-nm Ag MTPs), however, indicates that the holes preferentially started to appear and develop on the {111} facets of the particle with a decahedral or icosahedral structure (see Figure 4A and 4B, respectively), even though the {111} surface has the lowest energy relative to {100} and {110} surfaces.[25] This can probably be attributed to the existence of oxygen species at the boundaries between the tetrahedral units within each

decahedral and icosahedral MTPs. Various studies on Ag catalysts have concluded that a large amount of oxygen species can be dissolved in small Ag crystallites in the area of grain boundary defects and its adjacent defect planes.[30–32] Millar and co-workers also suggested that the presence of oxygen in those areas would induce a positive charge on the Ag atoms,[30] and these oxidized Ag would, in turn, act as a thin barrier to prevent the reaction between $HAuCl_4$ and Ag in those regions.

Once pits have been formed on the surface of Ag template, they will become the active sites for further replacement reaction. The Ag atoms in the interior will diffuse to the reaction sites and react with $HAuCl_4$ to generate Au atoms, which will be deposited on the surface of the Ag template. As shown in our previous studies, a nearly complete shell was formed on the surface of each Ag template when nanocubes and nanospheres with sizes >50 nm were subjected to the replacement reaction. This stage was not observed for the case of 11-nm Ag nanoparticles with a multiply twinned structure. This result is similar to the replacement reaction with Ag triangular nanoplates, where it was found that the nanoplate had to measure >20 nm in dimension along any axis in order to form a complete (or seamless) shell.[21a] Experimental and theoretical studies on the alloying of Ag/Au in nanoparticles has demonstrated that the rate of mixing between those two metals can be dramatically enhanced in the presence of vacancy defects.[33] As defined by the stoichiometric relationship between Ag and $HAuCl_4$, three Ag atoms will be consumed to form only one Au atom, leaving behind a huge number of vacancies in the template as the galvanic replacement reaction proceeds. These lattice vacancies will promote the migration of Ag and Au atoms significantly. In addition, Shibata and co-workers predicted that the vacancy-induced enhancement of rate of alloying also has a dependence on size, with faster alloying for smaller particles.[33] Mori and co-workers also found that the time scale for alloying between Cu and Au nanoparticles of 10 nm in diameter could be as short as a few seconds to minutes.[34] For 11-nm Ag MTPs with a decahedral shape, the dimension of each tetrahedral unit was only about 5 nm. Combining with the lattice strains induced by the twin defects at the boundaries, the diffusion of both Ag and Au atoms should be substantially enhanced. We believe the rapid diffusion of Au and Ag due to lattice vacancies, size effect, and boundary defects, hence the nearly instantaneous alloying between Au and Ag are responsible for the missing step of the formation of a complete shell on the Ag template during the replacement reaction.

The vacancies left behind by the migration of Ag and Au will diffuse and coalesce via an Ostwald ripening process to counter the increase of the total surface energy,[35] resulting in the enlargement of the surface openings on the particles and shrinkage of the ridges between the holes. At this stage, a nanocage with porous wall is formed from each Ag template, as illustrated in Figure 4C for a decahedron and icosahedron, respectively. After this stage, further addition of $HAuCl_4$ solution will reduce the thickness of the ridges and some of them will disappear or collapse due to dealloying, resulting in the formation of a ring-like structure with non-uniform wall thickness dependent on the angle of projection under TEM (see Figure 4C). However, these two stages, namely nanocage and nanoring, were not clearly separated. A mixture of nanorings and nanocages was always observed in the samples of hollow particles. By counting the number of identifiable nanorings and nanocages, the ratios of nanoring to nanocage were recorded for the particles obtained at different molar ratios of $HAuCl_4$ to Ag. At all reaction stages, the maximum ratio of nanoring to nanocage derived from the 11-nm Ag MTPs was ~2:1, while this maximum ratio decreased to ~1:3 for the 14-nm Ag nanoparticles. The reason that more nanocages were observed for the bigger Ag MTPs can be attributed to the stability of nanocages – bigger Ag nanoparticles would result in thicker ridges for the cages, which are more robust and will last longer than the smaller nanocages before evolving into nanorings with the progress of replacement reaction.

Similar to the dealloying process for Ag nanocubes and nanospheres with sizes >50 nm, the nanocages and nanorings derived from Ag MTPs will break into small pieces of solid particles rich of Au as the galvanic replacement reaction is allowed to continues (Figure 4C, step 4). Figure 2D shows TEM image of the final product corresponding to a reaction between11-nm Ag MTPs and 3.1 mL of $HAuCl_4$ solution.

Tuning of SPR Features

Figure 5A shows how the SPR spectra changed as the 11-nm Ag MTPs was titrated with 0.5 mM $HAuCl_4$ solution. The 11-nm Ag MTPs capped by oleylamine showed a sharp SPR peak at 400 nm, similar to the values reported for Ag nanoparticles in this size range.[10] As expected, the galvanic replacement reaction on the Ag nanoparticles caused a continuous red-shift for the SPR peak. With the addition of 1.0, 2.0, and 2.6 mL of $HAuCl_4$ solution, the SPR peak was positioned at 472, 565, and 616 nm, respectively (Figure 5A). While the SPR peak for nanocages derived from 100-nm Ag nanocubes could be tuned to 1200 nm in the near infrared region, the SPR peak of hollow nanostructures derived from 11-nm Ag MTPs stopped at 616 nm, primarily due to the small size of the structures and the large wall thickness relatively to the diameter of the template. After reacting with 3.1 mL of $HAuCl_4$ solution, the sample showed an SPR peak at 525 nm, corresponding to small piece of Au solid nanoparticles formed as a result of fragmentation of the hollow and highly porous structures.

For hollow nanostructures derived from 14-nm Ag MTPs, the SPR peak can be further tuned into the near infrared region. As shown in Figure 5B, the SPR peak continuously red-shifted to 740 nm as more $HAuCl_4$ solution was added. To better understand the SPR features, we used the DDA method to calculate the extinction spectra of Ag/Au alloy (2:1) nanorings with different outer diameters and ring thicknesses (Figure S4). In the model, the nanoring was simulated as a cylindrical ring with the height equal to the wall thickness (Figure S4 inset). It is interesting to note that such alloy nanorings with an outer diameter of 16 nm and a ring thickness of 3 nm in both axial and radial directions can have an optical resonant peak at 910 nm, indicating that the nanorings and nanocages in this size range are promising candidates for biomedical applications.

The Role of Oleylamine in the Galvanic Replacement Reaction

For a galvanic replacement reaction between Ag nanostructures and $HAuCl_4$ in an aqueous solution, the AgCl on the product side could be readily removed from the surface of the particles by refluxing the system thanks to the high solubility of AgCl in water at 100 °C.[21c] Otherwise, the AgCl would precipitate out and prevent the formation of Au/Ag alloy hollow nanostructures with uniform, homogeneous walls. When the reaction is carried out in an organic medium such as chloroform, the solubility of AgCl is much lower than that in boiling water. To minimize the interference of AgCl in the formation of Au/Ag alloy hollow structures, it is necessary to add extra oleylamine to the reaction system. This is because oleylamine can coordinate with Ag ions to form a complex, $AgCl(R\text{-}NH_2)_n$, soluble in the organic medium,[36] facilitating the separation of AgCl from the Ag template surface. Control experiment was also done to examine the effect of extra oleylamine on the morphology of resultant Au/Ag alloy hollow nanostructures. When no extra oleylamine was added before the galvanic replacement reaction, the color of the solution changed from yellow to brownish red after adding 2.6 mL of $HAuCl_4$ solution to the dispersion of Ag MTPs and black precipitate was found at the bottom of the flask. In contrast to the reaction carried out with the addition of extra oleylamine, no violet or blue color was observed. Figure 6A gives a typical TEM image of the product, showing very few hollow structures, while particles of several tens of nanometers in size dominated the sample. XRD patterns taken from the sample showed peaks from both AgCl and Au/Ag alloy (Figure 6B). The broad peaks of Au/Ag alloy and sharp peaks of AgCl indicate that the small particles in the sample were primarily made of Au/Ag alloy while the big ones were mainly

composed of AgCl. Without adding extra oleylamine, it is impossible to obtain Au/Ag alloy hollow nanostructures because the AgCl precipitate deposited on the surface of the template would prevent further reaction between $HAuCl_4$ and Ag. Even though the oleylamine capped on the surface of the Ag MTPs could enter into the solution phase and form complex with AgCl at the very beginning of the reaction, the surface-absorbed oleylamine would not be sufficient to complex with all AgCl as the replacement reaction proceeded. By adding extra oleylamine, the AgCl can be continuously transferred from the reaction sites on the template into the solution phase, completely eliminating the interference and contamination of AgCl during the formation Au/Ag alloy hollow nanostructures.

The Effect of Capping Ligand on the Galvanic Replacement Reaction

In addition to oleylamine, other organic surfactants such as oleic acid[10] and TOPO[37] have been widely used as capping ligands in the synthesis of Ag nanoparticles. As a result, it is important to know if the capping ligand will have any influence on the galvanic replacement reaction between $HAuCl_4$ and Ag nanoparticles in a specific solvent. To eliminate any difference that might arise from particle size and crystallinity, the Ag MTPs capped by oleic acid and TOPO were prepared through ligand exchange reactions with the oleylamine-capped Ag MTPs, rather than directly synthesized with those two surfactants.

Upon completion of the ligand exchange reaction and multiple times of washing to remove physically absorbed ligands, the Ag MTPs were examined with FTIR. As shown in Figure 7, each spectrum shows CH_2 and CH_3 symmetric and asymmetric stretching vibrations in the range of 2840 to 2950 cm^{-1} and CH_2 bending vibration at 1460 cm^{-1}, typical absorption bands for species with hydrocarbon groups. The FTIR of oleylamine-capped Ag MTPs showed a strong C-N stretching mode at 1384 cm^{-1}, an N-H bending mode at 1635 cm^{-1} and a weak band for N-H stretch at 3425 cm^{-1}, indicating the presence of oleylamine on the particle surface. The C-N stretch was blue-shifted from that of free amines (1000–1350 cm^{-1}), probably due to the interaction between N and Ag through coordination. After ligand exchange with oleic acid, the peaks for C-N and N-H stretch and bending disappeared, while two new bands at 1710 and 1370 cm^{-1}, corresponding to C=O stretch and symmetric COO^- stretch, respectively, were observed. These new peaks suggest a symmetric binding between the carboxylate head group and the Ag particle surface. The FTIR spectrum for TOPO-capped Ag MTPs showed P=O stretch at 1150 cm^{-1}, indicating the attachment of TOPO to the particle surface.

Figures 8A and 8B show TEM images of oleic acid-capped Ag MTPs before and after galvanic replacement reaction, respectively. The Ag nanoparticles capped with oleic acid appear identical to the initial oleylamine-capped MTPs in terms of shape and size. Both particles were spherical and the average diameter of the oleic acid-capped particles was 11.0 nm, almost the same as that of oleylamine-capped particles (11.2 nm). HRTEM image of the oleic acid-capped Ag MTPs (Figure 8C) revealed that the particles remained in the multiply twinned structure after ligand exchange. After galvanic replacement reaction with the same amount of 0.5 mM $HAuCl_4$ solution, the product obtained from oleic acid-capped Ag MTPs shows morphology completely different from those from oleylamine-capped MTPs. While hollow particles were obtained from the oleylamine-capped Ag MTPs, the galvanic replacement reaction with the oleic acid-capped templates did not yield any particles with voids in their interiors. The particles showed a rough surface and broad size distribution with an average diameter of 12.6±1.8 nm. Figure 8D shows a typical HRTEM image, displaying lattice fringes over the entire particle with no clear void. Although ~80% of the particles exhibited an increase in dimension as compared to the initial Ag MTPs, a few small fragments of broken particles with size ranging from 2 to 5 nm were present in the sample, similar to the collapsed hollow structures when oleylamine-capped Ag MTPss were reacted with 3.1 mL of 0.5 mM $HAuCl_4$. This result indicates that the reaction between $HAuCl_4$ and Ag probably only occurred on a limited number

of the oleic acid-capped particles, where the surface was not entirely covered. The lack of replacement reaction can be attributed to the inadequate access of $HAuCl_4$ to the Ag surface due to the strong adsorption of oleic acid on the template.

The adsorption of carboxylic acid on Ag surface has been extensively studied over the last several decades.[30,32,38,39] Bowden and Tabor assumed that reactive chemisorption of carboxylic acid on a Ag surface is hard to occur.[38] However, the good dispersity of the Ag particles capped with oleic acid in an organic solvent (after ligand exchange and removal of physically absorbed species) implies that the particles were well stabilized by oleic acid. The FT-IR of oleic acid-capped particles also showed a strong band of COO^- symmetric stretch at 1374 cm^{-1} and no absorption at 2400–3400 cm^{-1}, typical O-H stretch band for free carboxylic acids. Those results strongly indicate that the oleic acid was attached to the surface of Ag nanoparticles through chemical bonding. Ulman reported that the adsorption of alkanoic acid on a metal surface involves acid-base reaction driven by the formation of surface salt between carboxylate anion and surface metal cation.[40] Various studies have predicted that that the presence of adsorbed oxygen is a prerequisite to form a stable, chemisorbed species on a Ag single crystal surface.[30,41] It was also found that on AgO surface, the two oxygen atoms of carboxylate group bind to the surface nearly symmetrically,[40] consistent with the FT-IR of oleic acid-capped particles with strong symmetric COO^- stretch absorption relative to asymmetric stretch. All evidences indicate that the oleate species were formed on oleic acid-capped Ag nanoparticles, probably with the assistance of oxygen from air. The oleate species would impede the access of $HAuCl_4$ to Ag and thus block the galvanic replacement reaction. The Au atoms would deposit on the surface of Ag template non-epitaxically, inducing surface roughness and a slight increase of size. The formation of Au can still occur, however, due to possible reduction of $HAuCl_4$ by light and oleylamine.[42] Reaction could also occur between $HAuCl_4$ and some Ag MTPs whose surfaces were not completely covered with oleic acid due to fluctuation, resulting in the formation of few hollow particles. Overall, the number of hollow particles in the sample was less than 5% of the total oleic acid-capped Ag nanoparticles. The typical HRTEM of the particles after addition of $HAuCl_4$ solution (Figure 8D) shows that the particles were polycrystalline, and the MTP pattern could not be identified anymore due to the deposition of Au on the surface.

Silver nanoparticles with an average size of 8 nm were also directly synthesized with oleic acid serving as the capping ligand to examine the galvanic replacement reaction (Figure S5). Similar to the reaction that used Ag particles obtained from ligand exchange, few hollow particles were observed after the addition of $HAuCl_4$ solution.

Figures 8E and 8F show TEM images of TOPO-capped Ag MTPs before and after galvanic replacement reaction, respectively. TOPO, known to function as a relatively strong monodentate ligand in metal ion complexation, has a stronger interaction with Ag(I) in $CHCl_3$ than that of carboxylic acid.[43] While similar morphologies were observed for Ag MTPs capped with TOPO and those stabilized with oleylamine, the galvanic replacement reaction with TOPO-capped Ag MTPs did not yield any hollow structure. Particles with various sizes ranging from 2~20 nm were formed after adding $HAuCl_4$ solution, probably due to the coverage variation of TOPO on the surface of the Ag MTPs. Extensive reaction had taken place on the particles covered with less TOPO, while nearly no reaction occurred on the well-passivated nanoparticles.

4. Conclusion

We have investigated the galvanic replacement reaction between $HAuCl_4$ and small Ag nanoparticles with multiply twinned structures in chloroform to prepare hollow nanostructures made of Au/Ag alloys. By using oleylamine-capped Ag MTPs of 11 and 14 nm in diameter,

~12 and 15-nm polycrystalline hollow structures with 2–5 nm voids in their interiors were obtained, respectively. Based on the morphological evolution of the nanoparticles, we proposed that the oxidation of Ag started from the {111} facets of an MTP, even though lattice defects of high surface energy exist at the gaps between the tetrahedral units of the particle. In stead of forming a complete shell, the replacement reaction on Ag MTPs resulted in Au/Ag alloy nanorings and nanocages. This can be attributed the rapid alloying between Ag and Au as caused by *i*) the high density of vacancies generated by the replacement of Ag with Au at a mole ratio of 3:1 (Ag:Au); *ii*) the rich lattice defects at the grain boundaries within the MTPs; and *iii*) the small size of the particles, and thus significantly enhanced diffusion of the metal atoms. The SPR peaks could be tuned to 616 nm for the hollow nanoparticles derived from 11-nm Ag MTPs and to 740 nm for the 14-nm Ag MTPs, respectively.

Oleylamine plays an important role in the formation of Au/Ag alloy hollow nanostructures through a galvanic replacement. Unlike the reaction carried out in an aqueous solution where the AgCl formed from the oxidation of Ag by $HAuCl_4$ can be dissolved by refluxing the system, the reaction in an organic medium relies on oleylamine to transfer AgCl from the template surface into the solvent by forming a soluble complex. Without adding extra oleylamine, one can only obtain irregularly shaped particles contaminated with AgCl solid. The capping ligand on the surface of Ag MTPs also significantly affects a galvanic replacement reaction as well as the morphology of the product. Hollow nanoparticles were not obtained from oleic acid and TOPO-capped Ag MTPs, probably due to the strong interaction between oleic acid and Ag surface via the formation of carboxylate in the presence of oxygen or through complexation between Ag and the oxygen of TOPO.

Supplementary Material

Refer to Web version on PubMed Central for supplementary material.

Acknowledgements

This work was supported in part by the NIH (R01CA120480), the NSF (DMR-0451788), and a Fellowship from the David and Lucile Packard Foundation. Y.X. is a Camille Dreyfus Teacher Scholar (2002–2007). Z.Y.L. was supported by the National Key Basis Research Special Foundation of China (No. 2004 CB719804). Part of the work was performed at the Nanotech User Facility, a member of the National Nanotechnology Infrastructure Network (NNIN) funded by the NSF. H.-Y.T. and B.A.K. thank the Robert A. Welch Foundation for financial support.

References

1. (a) Sanders AW, Routenberg DA, Wiley BJ, Xia YN, Dufresne ER, Reed MA. Nano Lett 2006;6:1822. [PubMed: 16895380] (b) Tao A, Sinsermsuksakul P, Yang PD. Angew Chem-Int Edit 2006;45:4597.
2. Chen SW, Yang YY. J Am Chem Soc 2002;124:5280. [PubMed: 11996564]
3. Teng XW, Black D, Watkins NJ, Gao YL, Yang H. Nano Lett 2003;3:261.
4. Tessier PM, Velev OD, Kalambur AT, Rabolt JF, Lenhoff AM, Kaler EW. J Am Chem Soc 2000;122:9554.
5. Imura R, Koyanagi H, Miyamoto M, Kikukawa A, Shintani T, Hosaka S. Microelectron Eng 1995;27:105.
6. Hasobe T, Imahori H, Kamat PV, Ahn TK, Kim SK, Kim D, Fujimoto A, Hirakawa T, Fukuzumi S. J Am Chem Soc 2005;127:1216. [PubMed: 15669861]
7. (a) Xia YN, Yang PD, Sun YG, Wu YY, Mayers B, Gates B, Yin YD, Kim F, Yan YQ. Adv Mater 2003;15:353. (b) Sun YG, Yin YD, Mayers BT, Herricks T, Xia YN. Chem Mat 2002;14:4736. (c) Sun YG, Xia YN. Adv Mater 2002;14:833. (d) Sun YG, Gates B, Mayers B, Xia YN. Nano Lett 2002;2:165. (e) Hong BH, Bae SC, Lee CW, Jeong S, Kim KS. Science 2001;294:348. [PubMed: 11546837] (f) Jana NR, Gearheart L, Murphy CJ. Chem Commun 2001:617. (g) Kondo Y, Takayanagi K. Science 2000;289:606. [PubMed: 10915620]

8. (a) Busbee BD, Obare SO, Murphy CJ. Adv Mater 2003;15:414. (b) Jiang XC, Brioude A, Pileni MP. Colloid Surf A-Physicochem Eng Asp 2006;277:201. (c) Park HJ, Ah CS, Kim WJ, Choi IS, Lee KP, Yun WS. J Vac Sci Technol A 2006;24:1323. (d) Hofmeister H, Nepijko SA, Ievlev DN, Schulze W, Ertl G. J Cryst Growth 2002;234:773.
9. Brust M, Walker M, Bethell D, Schiffrin DJ, Whyman R. J Chem Soc-Chem Commun 1994:801.
10. Lin XZ, Teng XW, Yang H. Langmuir 2003;19:10081.
11. Wiley B, Sun YG, Mayers B, Xia YN. Chem-Eur J 2005;11:454.
12. (a) Sun YG, Xia YN. Science 2002;298:2176. [PubMed: 12481134] (b) Yu DB, Yam VWW. J Am Chem Soc 2004;126:13200. [PubMed: 15479055] (c) Im SH, Lee YT, Wiley B, Xia YN. Angew Chem-Int Edit 2005;44:2154. (d) Huang CJ, Chiu PH, Wang YH, Chen WR, Meen TH. J Electrochem Soc 2006;153:D129.
13. (a) Chen SH, Fan ZY, Carroll DL. J Phys Chem B 2002;106:10777. (b) Chen SH, Carroll DL. J Phys Chem B 2004;108:5500. (c) Umar AA, Oyama M. Cryst Growth Des 2006;6:818. (d) Sun YA, Xia YN. Adv Mater 2003;15:695. (e) Sun YG, Mayers B, Xia YN. Nano Lett 2003;3:675.
14. Selvakannan PR, Sastry M. Chem Commun 2005:1684.
15. (a) Loo C, Lin A, Hirsch L, Lee MH, Barton J, Halas N, West J, Drezek R. Technol Cancer Res Treat 2004;3:33. [PubMed: 14750891] (b) Shukla S, Priscilla A, Banerjee M, Bhonde RR, Ghatak J, Satyam PV, Sastry M. Chem Mat 2005;17:5000.
16. Schwartzberg AM, Oshiro TY, Zhang JZ, Huser T, Talley CE. Anal Chem 2006;78:4732. [PubMed: 16808490]
17. (a) Chen J, Saeki F, Wiley BJ, Cang H, Cobb MJ, Li ZY, Au L, Zhang H, Kimmey MB, Li XD, Xia Y. Nano Lett 2005;5:473. [PubMed: 15755097] (b) Chen JY, Wiley B, Li ZY, Campbell D, Saeki F, Cang H, Au L, Lee J, Li XD, Xia YN. Adv Mater 2005;17:2255. (c) Chen JY, McLellan JM, Siekkinen A, Xiong YJ, Li ZY, Xia YN. J Am Chem Soc 2006;128:14776. [PubMed: 17105266]
18. Oldenburg SJ, Averitt RD, Westcott SL, Halas NJ. Chem Phys Lett 1998;288:243.
19. Graf C, van Blaaderen A. Langmuir 2002;18:524.
20. Lu Y, Yin YD, Li ZY, Xia YA. Nano Lett 2002;2:785.
21. (a) Sun YG, Mayers B, Xia YN. Adv Mater 2003;15:641. (b) un YG, Xia YN. Nano Lett 2003;3:1569. (c) Sun YG, Xia YN. J Am Chem Soc 2004;126:3892. [PubMed: 15038743] (d) Sun YG, Wiley B, Li ZY, Xia YN. J Am Chem Soc 2004;126:9399. [PubMed: 15281832] (e) Sun YG, Xia YN. Adv Mater 2004;16:264. (f) Sun YG, Mayers BT, Xia YN. Nano Lett 2002;2:481.
22. Yang J, Lee JY, Too HP. J Phys Chem B 2005;109:19208. [PubMed: 16853479]
23. Yin Y, Erdonmez C, Aloni S, Alivisatos AP. J Am Chem Soc 2006;128:12671. [PubMed: 17002360]
24. Liang HP, Zhang HM, Hu JS, Guo YG, Wan LJ, Bai CL. Angew Chem-Int Edit 2004;43:1540.
25. Wang ZL. J Phys Chem B 2000;104:1153.
26. Harfenist SA, Wang ZL, Whetten RL, Vezmar I, Alvarez MM. Adv Mater 1997;9:817.
27. Ino S. J Phys Soc Jpn 1966;21:346.
28. (a) Marks LD. Rep Prog Phys 1994;57:603. (b) Tamaru K. Trans Faraday Soc 1959;55:824.
29. Wang ZL, Ahmad TS, ElSayed MA. Surf Sci 1997;380:302.
30. Millar GJ, Metson JB, Bowmaker GA, Cooney RP. J Catal 1994;147:404.
31. (a) Meima GR, Knijff LM, Vis RJ, Vandillen AJ, Vanburen FR, Geus JW. J Chem Soc-Faraday Trans I 1989;85:269. (b) Wu K, Wang DZ, Wei XM, Cao YM, Guo XX. J Catal 1993;140:370.
32. Lefferts L, Vanommen JG, Ross JRH. Appl Catal 1987;31:291.
33. Shibata T, Bunker BA, Zhang Z, Meisel D, Vardeman CF II, Gezelter JD. J Am Chem Soc 2002;124:11989. [PubMed: 12358545]
34. Mori H, Komatsu M, Takeda K, Fujita H. Philos Mag Lett 1991;63:173.
35. Sieradzki K. J Electrochem Soc 1993;140:2868.
36. McDougall GJ, Hancock RD. J Chem Soc-Dalton Trans 1980:654–658.
37. Saponjic ZV, Csencsits R, Rajh T, Dimitrijevic NM. Chem Mat 2003;15:4521.
38. Bowden, FP.; Tabor, D. The Friction and Lubrication of Solids. Oxford University Press; Oxford, UK: 2000.

39. (a) Schlotter NE, Porter MD, Bright TB, Allara DL. Chem Phys Lett 1986;132:93. (b) Firment LE, Somorjai GA. J Vac Sci Tech 1980;17:574. (c) Yanase A, Komiyama H, Tanaka K. Surf Sci 1990;226:L65. (d) Millar GJ, Seakins J, Metson JB, Bowmaker GA, Cooney RP. Chem Commun 1994:525. (e) Jovic BM, Drazic DM, Jovic VD. J Serbian Chem Soc 1998;63:793.

40. Ulman A. Chem Rev 1996;96:1533. [PubMed: 11848802]

41. Barteau MA, Bowker M, Madix RJ. Surf Sci 1980;94:303.

42. Kuo PL, Chen CC. Langmuir 2006;22:7902. [PubMed: 16922581]

43. Sekine T, Takahashi Y. Bullet Chem Soc J 1973;46:1183.

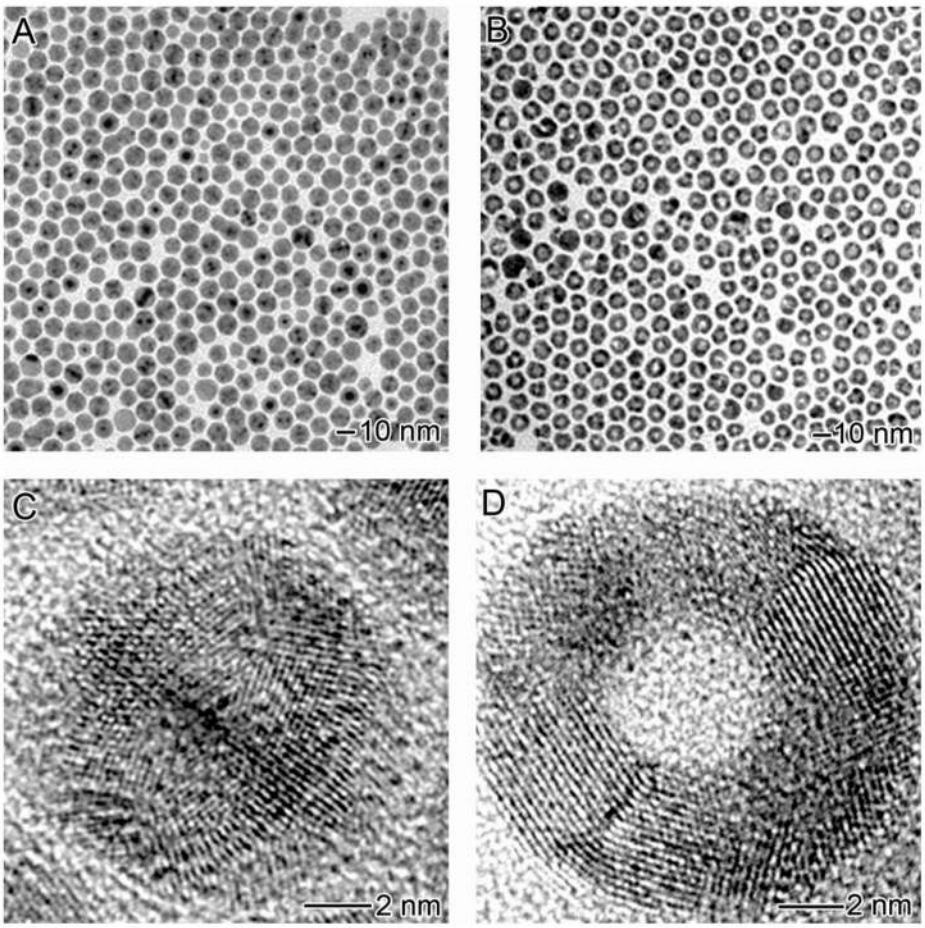

Figure 1.

(A) TEM image of Ag nanoparticles prepared with oleylamine as the capping ligand. (B) TEM image of hollow nanoparticles obtained by adding 2.6 mL $HAuCl_4$ (0.5 mM) to react with the Ag nanoparticles in $CHCl_3$. (C) HRTEM of a Ag nanoparticle with icosahedral shape. (D) HRTEM of a hollow nanoparticle formed via the galvanic replacement reaction.

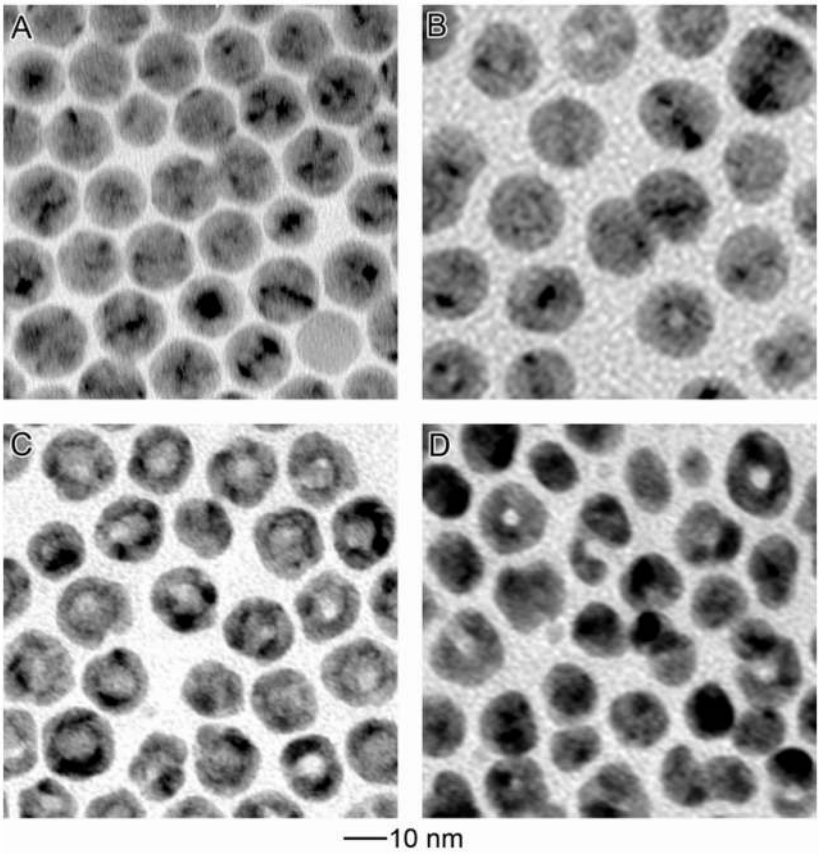

Figure 2.
Morphological evolution for Ag nanoparticles capped with oleylamine (A) before and after reacting with (B) 1.0 mL, (C) 2.0 mL, and (D) 3.1 mL of 0.5 mM $HAuCl_4$ in $CHCl_3$.

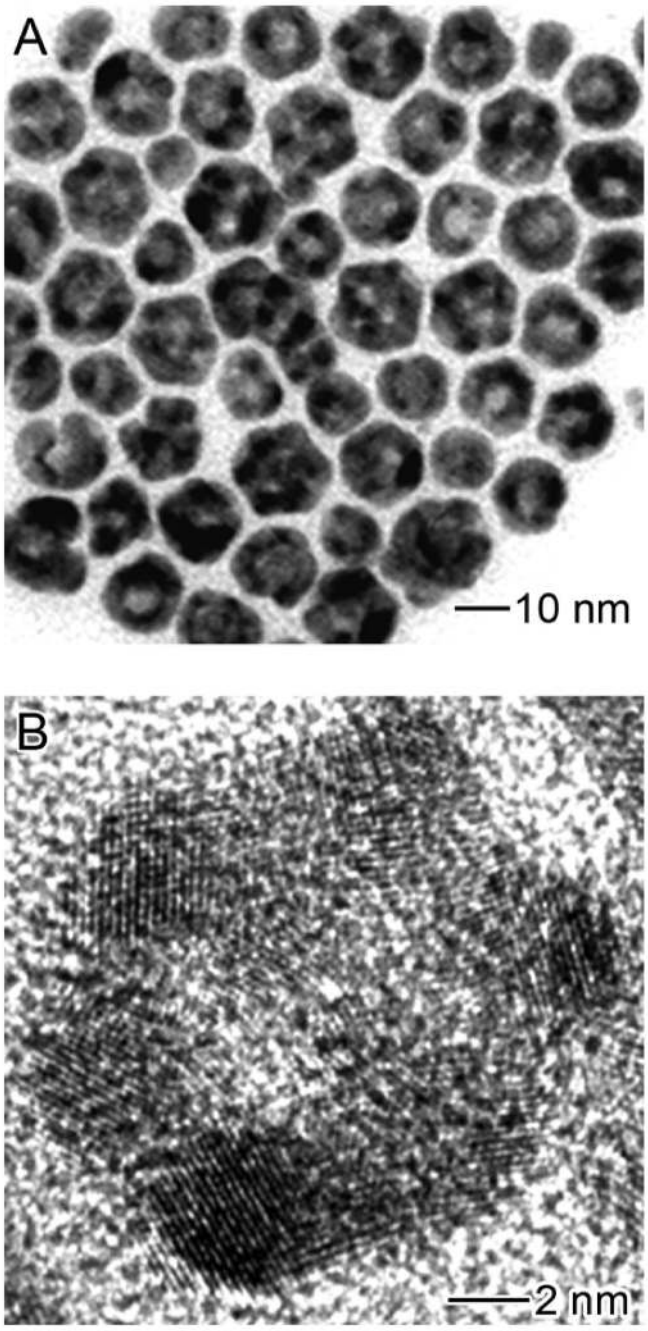

Figure 3.
(A) Nanocages derived from 14.0-nm Ag nanoparticles by reacting with 1.2 mL of 0.5 mM $HAuCl_4$ in $CHCl_3$. The average size of the hollow particles increased to 15.1±2.1 nm. A majority of the particles exhibit the cage-like morphology. (B) HRTEM of a nanocage. Note that the lattice fringes are missing in some regions, corresponding to holes on the surface.

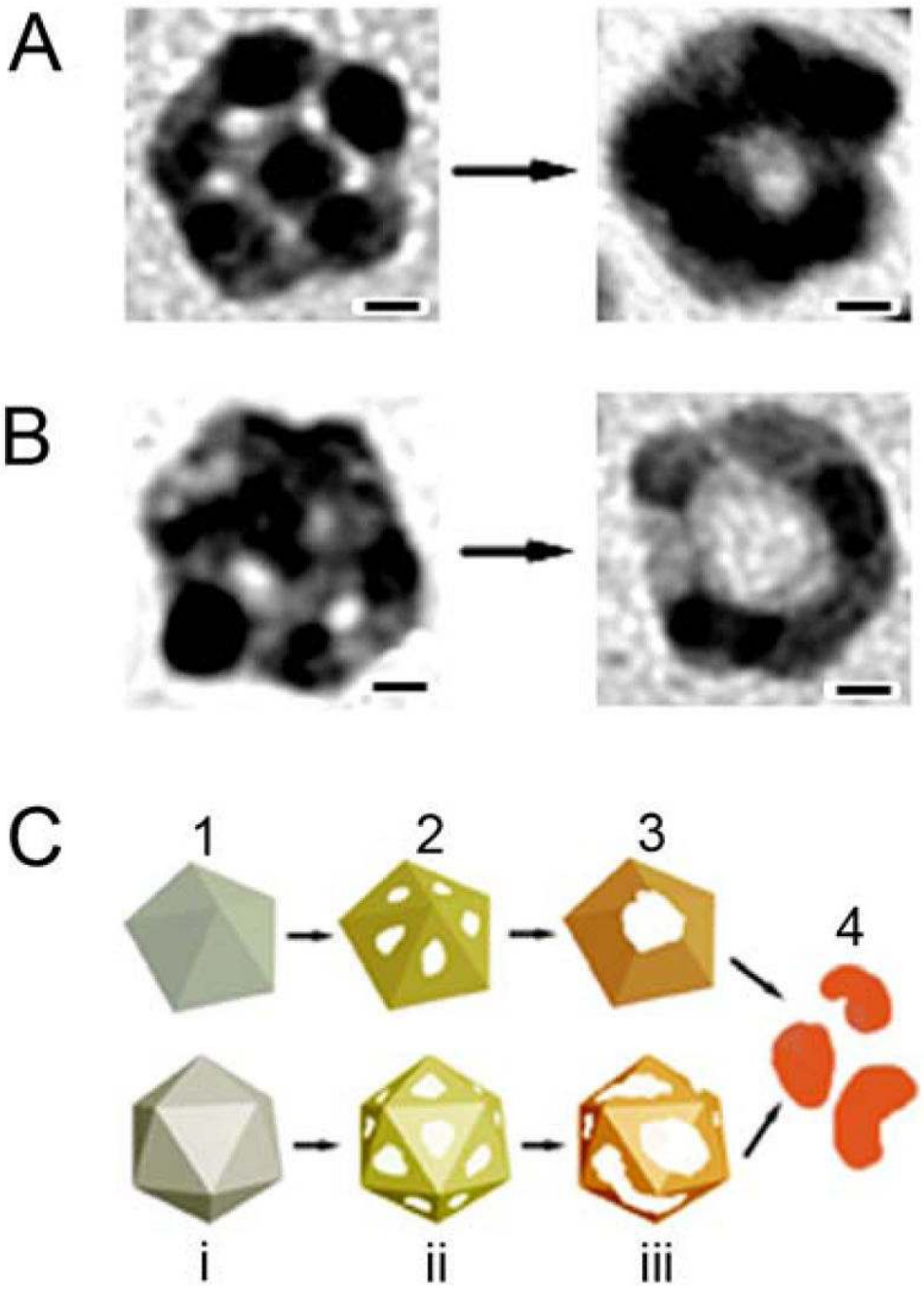

Figure 4.

Morphological evolution for Ag MTPs with a (A) decahedral and (B) icosahedral structure during the galvanic replacement reaction. Holes on {111} facets of the particle were clearly resolved. As the reaction proceeded, these holes eventually disappeared. In stead, a big void was formed in the middle of the particle. (C) Mechanisms proposed to account for the formation of hollow structures from oleylamine-capped Ag MTPs. When $HAuCl_4$ in $CHCl_3$ is injected to the Ag MTPs, pitting starts from the surfaces of the nanoparticles to form pinholes which make the particles appear like nanocages (step 2). As the reaction proceeds, some ridges break due to consumption of the Ag and some grow through the deposition of Au and Oswald ripening. Pinholes combine and form a big opening on the particles – the shape of the hollow

particles evolves from nanocage into nanoring (step 3). Adding more $HAuCl_4$ after this stage would result in the collapse of the hollow particles and formation of small fragments (step 4). As the ratio of $HAuCl_4$ to Ag increased from step (1) to step (4), the compositional change from pure Ag to Ag-Au alloys is illustrated by different colors. The scale bars for (A) and (B) are 2 nm.

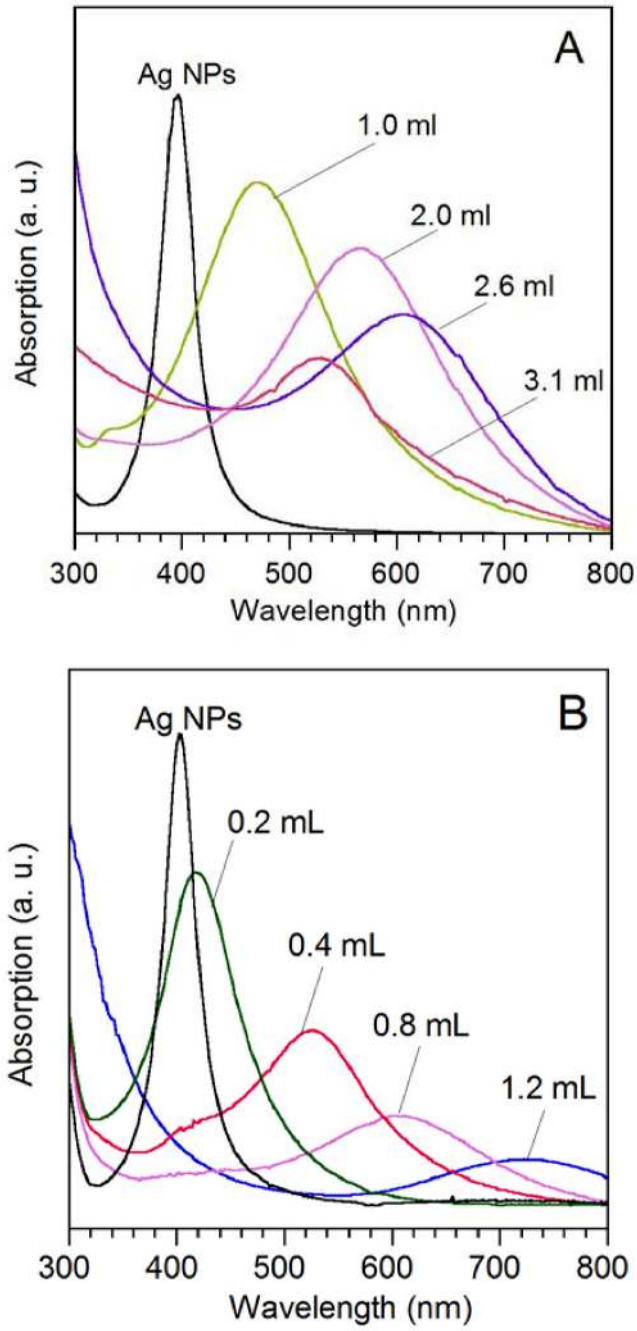

Figure 5.

UV-vis extinction spectra taken from the suspension of oleylamine-capped Ag MTPs in $CHCl_3$ after different volumes of 0.5 mM $HAuCl_4$ had been added. The SPR peaks were positioned at 400 and 404 nm for the 11 and 14 nm Ag MTPs, respectively. (A) After adding 1.0, 2.0, 2.6 and 3.1 mL of $HAuCl_4$ solution to the 11-nm Ag MTPs, the SPR peak was shifted to 472, 565, 616, and 525 nm, respectively. (B) After adding 0.2, 0.4, 0.8 and 1.2 mL of $HAuCl_4$ solution to the 14-nm Ag MTPs, the SPR peak was shifted to 422, 532, 614, and 740 nm, respectively.

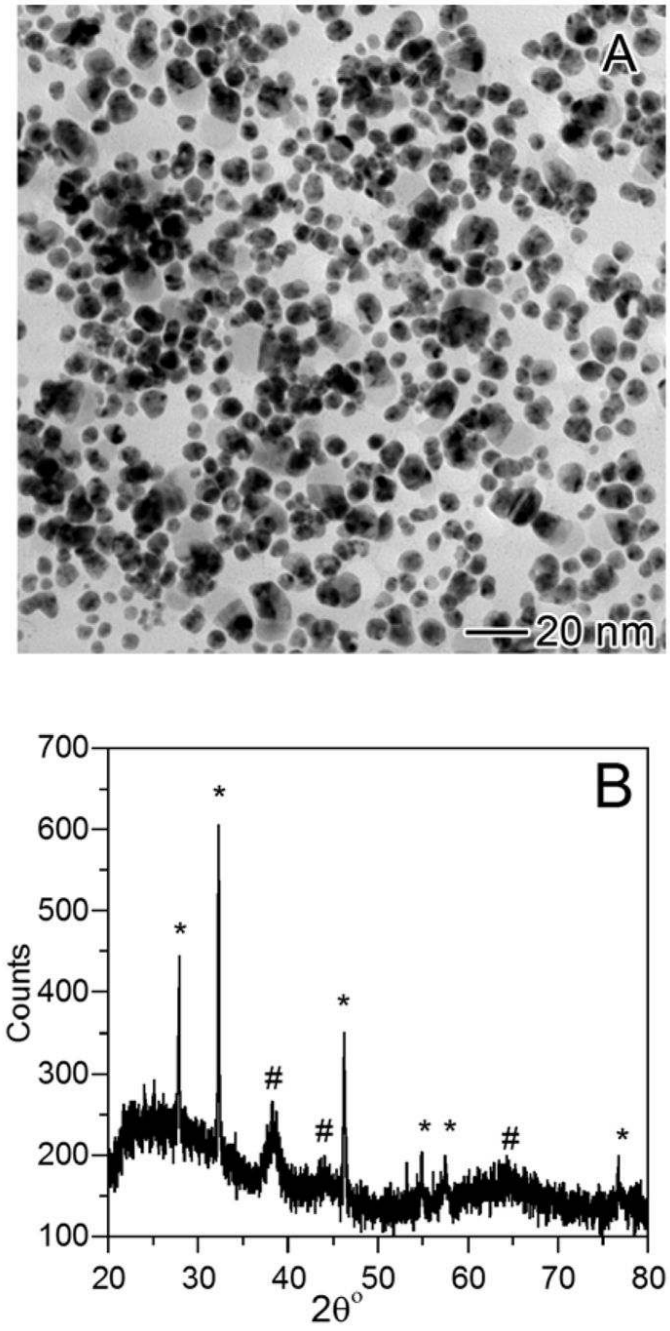

Figure 6.

Galvanic replacement reaction between $HAuCl_4$ and oleylamine-capped Ag MTPs without adding extra oleylamine: (A) TEM image showing a mix of few hollow particles and a lot of irregularly shaped large particles. (B) XRD of the sample revealing the coexistence of peaks for both Ag-Au alloy (#) and AgCl (*).

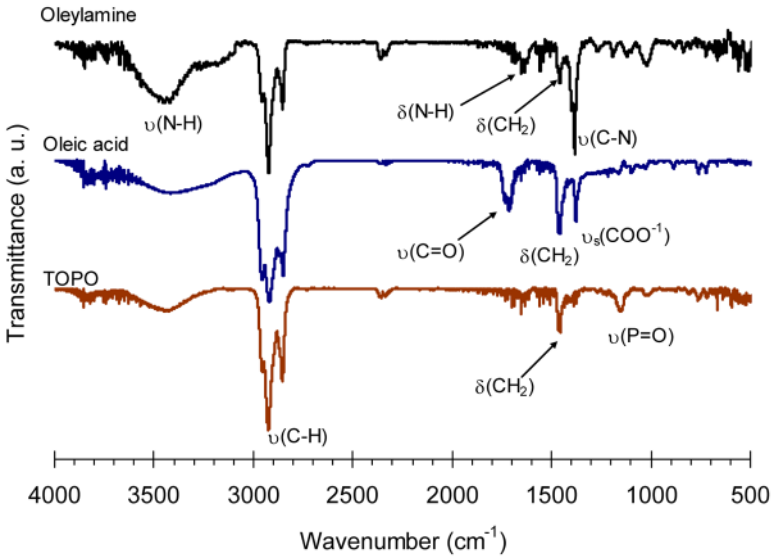

Figure 7.

FT-IR spectra of Ag nanoparticles capped with different ligands. The particles were initially made with oleylamine as the capping ligand and then exchanged with oleic acid and TOPO, respectively.

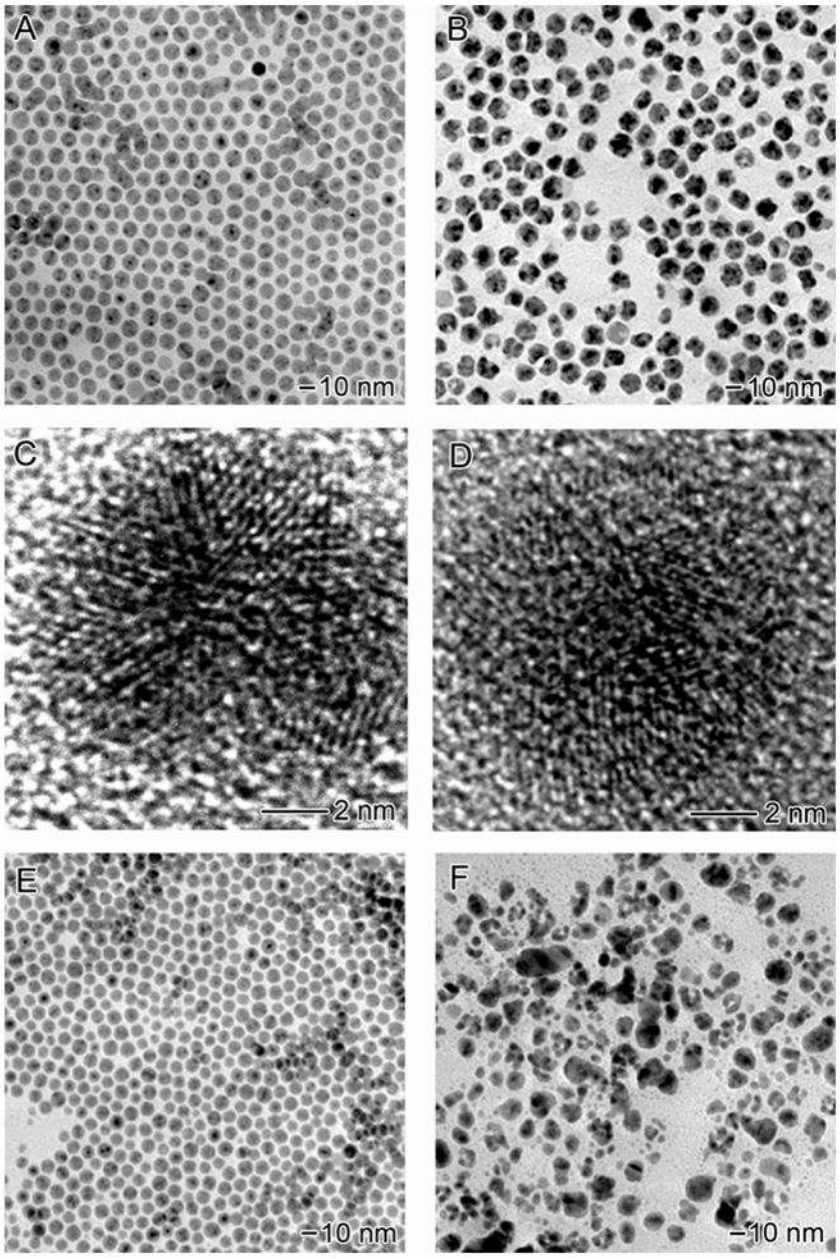

Figure 8.

The morphology of product is strongly dependent on the capping ligand. The Ag MTPs were made with oleylamine as the capping ligand. After ligand exchange, they were capped with (A) oleic acid and (E) TOPO, respectively. When reacted with 2.6 mL of 0.5 mM $HAuCl_4$, few hollow particles were observed for (B) oleic acid-capped and (F) TOPO-capped Ag nanoparticles and the majority of the particles turned from spherical to irregular shapes. (C, D) HRTEM images of Ag nanoparticles capped with oleic acid before and after the replacement reaction. The oleic acid-capped Ag nanoparticles also had a MTP structure. After replacement reaction, the MTP pattern cannot be identified any more.